Neutron scattering evidence on the nature of the boson peak

2007 J. Phys.: Condens. Matter 19 205106

(http://iopscience.iop.org/0953-8984/19/20/205106)

IOP PUBLISHING JOURNAL OF PHYSICS: CONDENSED MATTER

J. Phys.: Condens. Matter **19** (2007) 205106 (15pp) doi:10.1088/0953-8984/19/20/205106

Neutron scattering evidence on the nature of the boson peak

U Buchenau[1], A Wischnewski[1], M Ohl[1] and E Fabiani[2]

[1] Institut für Festkörperforschung, Forschungszentrum Jülich, Postfach 1913, D-52425 Jülich, Federal Republic of Germany
[2] Institute Laue-Langevin, BP 156, F-38042 Grenoble Cedex 9, France

E-mail: buchenau-juelich@t-online.de

Received 9 October 2006
Published 25 April 2007
Online at stacks.iop.org/JPhysCM/19/205106

Abstract

Literature and unpublished neutron spectra of seven classical glass formers in the boson peak region are evaluated in terms of eigenvalue densities. The boson peak translates into a true maximum of the eigenvalue density, lying about a factor of two higher than the boson peak eigenvalue and followed by a slow decrease towards higher eigenvalues.

We interpret the data in terms of a crossover from sound waves at low eigenvalues to a more or less constant eigenvalue density at high eigenvalues. The Ioffe–Regel limit of strong sound wave damping lies at the crossover eigenvalue λ_c, slightly higher than the boson peak. A four-parameter fit form based on the soft-potential model provides reasonable fits up to and including the beginning of the slow decrease. The parameters from the neutron data agree within their error bars with those determined from the low-temperature anomalies in the heat capacity and in the thermal conductivity. The results indicate that the strong scattering of sound waves in glasses is due to the interaction with the excess vibrational modes.

1. Introduction

There is as yet no generally accepted explanation of the boson peak in the neutron or Raman spectrum of glasses. The boson peak is a broad peak at an energy transfer of a few meV, where simple crystals have only sound waves. Glasses seem to have a sizable amount of excess vibrations at this boson peak. At present, it is not clear which driving force brings these vibrations down into the low-frequency region, though there are several possible explanations [1–8]. Another controversial question [9, 10] is whether the interaction with these vibrations is the physical reason for the Ioffe–Regel limit, the strong scattering of sound waves in the terahertz range.

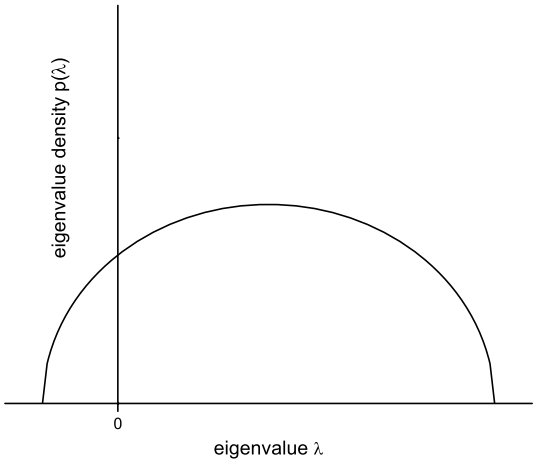

Figure 1. The Wigner semicircle [11] expectation for a glass.

In this paper, we present neutron spectra of seven heavily studied glasses in terms of eigenvalue densities. The eigenvalue is the square of the frequency. Since the neutron measurement supplies the frequency as energy transfer $E = \hbar\omega$, we define the eigenvalue $\lambda = E^2$ and measure it in meV^2. The eigenvalue density $p(\lambda) = g(E)/2E$, where $g(E)$ is the conventional vibrational density of states.

The choice of the eigenvalue as the independent variable rather than the frequency has several advantages. Experimentally, the boson peak is a broad peak in $g(E)/E^2$. Therefore it should be only a shoulder in $p(\lambda)$. But we will see that there is a true maximum in $p(\lambda)$ itself in all these glasses and at all temperatures, persisting into the temperature range of the undercooled liquid.

From a theoretical point of view, the eigenvalue is also a good choice. Figure 1 illustrates the theoretical problem posed by the boson peak. In glasses, one has force constant disorder and hence a random dynamical matrix. The eigenvalue density of such a random matrix is the Wigner semicircle [11] shown in figure 1. Since the short-range order of the glass is not too far away from that of the crystal, one expects the centre of the semicircle to be close to the lowest van Hove singularity of the crystal. If the disorder is strong enough, the circle will extend below the eigenvalue zero into the region of instability. The theoretical problem lies in dealing with these instabilities.

At present, there is no satisfactory theoretical treatment of the full problem. There is a one-parameter theory which ignores the instabilities and introduces shear modulus disorder into a stable solid [12]. The parameter characterizes the strength of the disorder and is limited by the stability condition. The theory explains the strong sound-wave damping at the boson peak in an experimentally satisfactory and theoretically appealing way. Introducing the tunnelling state scattering by hand (a usual procedure for classical theories), it is even able to reproduce the full thermal conductivity curve of the glass, including the rise after the plateau. The theory provides a natural crossover from a sound-wave density of states at low frequency to a Wigner semicircle at high frequency.

The theory predicts only an excess of at most a factor of two over the Debye value at the peak. Many glasses show a higher excess factor, maybe due to optical modes which are not taken into account by the theory, but possibly also due to the neglect of the negative eigenvalues.

These negative eigenvalues exist in the glass, as demonstrated by the two-level states at low temperature [13]. Therefore the theory might be incomplete at low eigenvalues.

A well-developed treatment of the whole neighbourhood of the eigenvalue zero in figure 1 is the soft-potential model. It requires three parameters: the density P_s of the excess modes, the zero-point energy W in the purely quartic potential, and the coupling C between sound waves and excess modes. The soft-potential model has been found to be able to describe the mixture of sound waves, resonant vibrational and relaxational modes at low frequency, below the boson peak [14, 15]. The model has been extended [1], describing the boson peak in terms of the elastic interaction between excess modes. But this new development fails to describe the crossover to a Wigner-type solution at higher frequencies. The measurements demonstrate that one needs such a crossover.

In view of these deficiencies of available theories, we decided to use a pragmatic description to fit our data. This description uses the classical soft-potential model at low frequency and puts in a crossover to a Wigner-type solution at higher frequencies by hand. We begin in section 2 with the data, their evaluation and their transformation into an eigenvalue density. Section 3 describes and motivates their fit in terms of our pragmatical fit form, able to describe the crossover from a mixture of sound waves, relaxations and resonant modes at low frequency to a slowly decreasing eigenvalue density at high frequency. The fit results, their relation to the low-temperature anomalies of glasses [13, 14] and their relation to the Ioffe–Regel limit are discussed in section 4. Section 5 summarizes and concludes the paper.

2. Neutron data

All measurements presented in this section were performed on the time-of-flight spectrometer IN6 at the High Flux Reactor of the Institute Laue-Langevin in Grenoble, France. The wavelength of the incoming neutrons was 4.1 Å. Most of the data have already been published, but not in the scaling presented here. The samples had a scattering probability of about 10% to provide a reasonable balance between signal strength and multiple scattering contamination.

The data were evaluated in a new scheme for the determination of the vibrational density of states from coherent and incoherent inelastic neutron scattering data, developed by two of us at the Institute Laue-Langevin in Grenoble [16].

Figure 2 shows the classical case of silica, the glass spectra at 155 and 1104 K [18] and the crystal spectrum from a lattice dynamical calculation [17]. In the region around 10 meV, the crystal shows pronounced van Hove singularities. The disorder should broaden these low-lying van Hove singularities into a semi-circle on the basis of Wigner's solution [11] of the random-matrix problem. Instead, the glass shows a maximum at a lower frequency, followed by a slow decrease toward higher eigenvalues.

The boson peak of silica shifts strongly to higher frequency with increasing temperature, contrary to the usual behaviour of the boson peak in other glasses and implying an improbably high negative mode Grüneisen parameter. We will discuss a possible physical origin of this unusual behaviour in section 4.

While the temperature behaviour of silica is unusual, the spectral shape is not. Judging from the literature, the broad eigenvalue density maximum above the boson peak eigenvalue seems to be a universal glass feature. In $g(E)/E^2$, one finds a stronger than $1/E$-decrease above the boson peak in a metallic glass [19] as well as in the molecular glasses OTP [20] and glycerol [21]. This decrease is even more pronounced in the translational motion of a guest molecule [22]. In low-temperature heat capacity (C_p) data, there is a stronger than $1/T$ decrease in C_p/T^3 with increasing temperature T, as seen in both glassy and orientationally disordered ethanol [23]. The universal decrease of the eigenvalue density is also observed in cluster simulations [24].

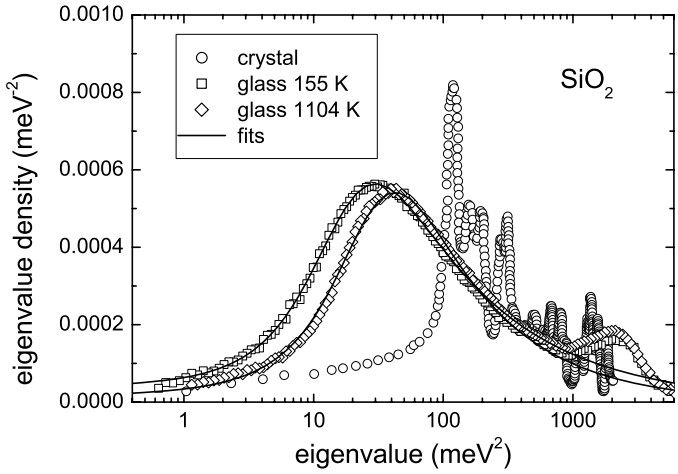

Figure 2. Eigenvalue density in crystalline α-quartz [17] and in vitreous silica [18], plotted against the eigenvalue on a logarithmic scale. The lines are fits in terms of equation (4).

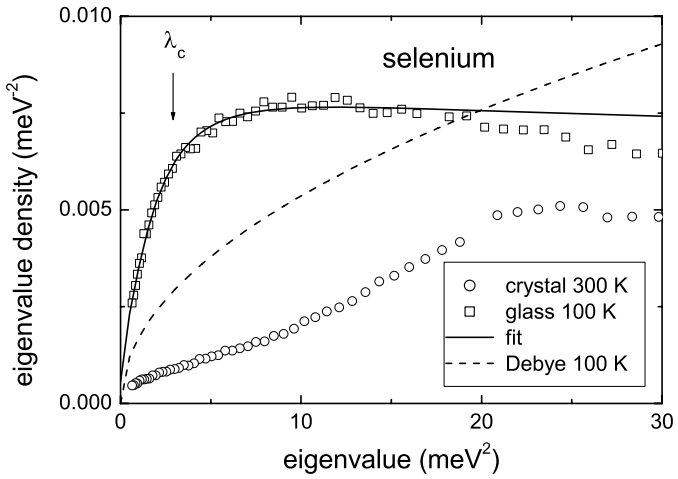

Figure 3. Eigenvalue density in crystalline and glassy selenium [25]. The continuous line is a fit in terms of equation (4); the dashed line shows the sound-wave fraction at 100 K according to the Debye model. The arrow denotes the fitted crossover eigenvalue λ_c from sound waves to excess modes.

Figure 3 shows the eigenvalue density of glass and crystal in another well-studied case, selenium [25], on a linear eigenvalue scale. Amorphous selenium has a relatively high sound-wave density (a factor of three higher than the crystal) and a relatively low density of additional modes. If one extrapolates the Debye sound-wave density of states to higher frequencies, it already exceeds the measured density of states at about 20 meV^2, an energy transfer of 4.5 meV, which is only half the Debye limit of 9.6 meV. The example illustrates the importance of dealing correctly with the fate of the sound waves at higher eigenvalues. Obviously, one needs an effective cutoff of the Debye density of states at an eigenvalue close to the one corresponding

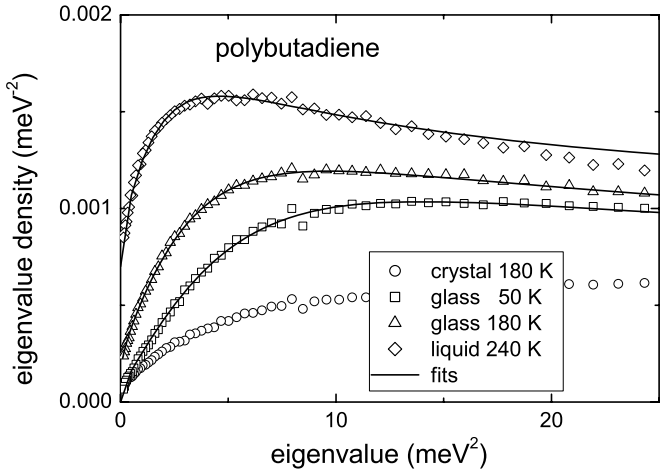

Figure 4. Eigenvalue density in crystalline, glassy and liquid polybutadiene [26]. Lines are fits in terms of equation (4).

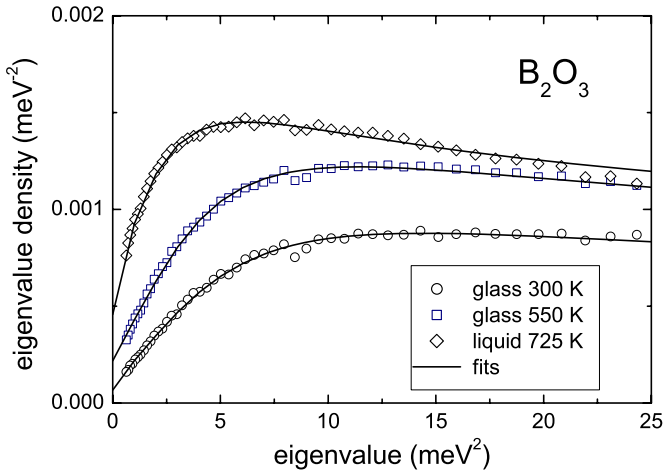

Figure 5. Eigenvalue density in glassy and liquid B_2O_3 [27]. Lines are fits in terms of equation (4).

to the boson peak. Our fit in terms of an appropriate interpolation form, equation (4), contains such a cutoff in terms of a crossover eigenvalue λ_c, denoted by the arrow in figure 3.

Polybutadiene in figure 4 shows the usual temperature behaviour, a downward shift of the maximum in $p(\lambda)$ with increasing temperature. According to the fits, most of this shift is due to the decrease in the Debye frequency and the increase in the relaxational component, while the crossover eigenvalue remains unchanged nearly up to the glass transition.

B_2O_3 in figure 5 shows again an unusual temperature behaviour. Below 300 K, one has essentially a temperature-independent eigenvalue density. Then the maximum increases markedly up to 550 K (the glass temperature), with only a small shift of the maximum to lower values. Above the glass transition, the maximum shifts markedly to lower values. We will come back to this unusual behaviour in the discussion.

3. The modelling of the spectra

We choose to fit our data in terms of a pragmatic fit form for a crossover at the boson peak. At lower frequency, we use the soft-potential description [14, 15] of a mixture of sound waves with resonant vibrational or relaxational modes. Above the boson peak, we assume a more or less constant eigenvalue density resulting from a random dynamical matrix. We follow the theoretical convention of normalizing the eigenvalue density to one. If one wants the real number of modes per atom, one has to multiply the given numbers by the factor three.

At low frequency, one has an elastic medium with well-defined sound waves coexisting with a small number of additional modes: resonant vibrational modesas well as relaxational modes. There, the neutron spectra should be well described by the soft-potential expression for the effective eigenvalue density

$$p(\lambda) = \frac{3}{2}\frac{\lambda^{1/2}}{(\hbar\omega_D)^3} + f_{vib}\lambda^{3/2} + f_{rel}. \tag{1}$$

This expression for the low-frequency spectrum is derived from the soft-potential model [14], an extension of the tunnelling model of the low-temperature anomalies of glasses. The first term contains the Debye frequency ω_D and describes the sound waves. In addition to the sound waves, the model postulates a continuous distribution of additional modes around the eigenvalue zero. The positive eigenvalues provide vibrational resonant modes coexisting with the sound waves, the second term of equation (1). The negative eigenvalues, in principle unstable modes, are supposed to be stabilized by the anharmonic fourth-order term of the mode potential. They lead to double-well potentials, giving rise to tunnelling states at low temperatures and to classical relaxation at higher temperatures. The third term of equation (1) is the soft-potential expectation for this classical relaxation spectrum. f_{vib} and f_{rel} are given in terms of the parameters of the soft-potential model [15]

$$f_{vib} = \frac{P_s M}{48}\left(\frac{1}{W}\right)^5 \tag{2}$$

and

$$f_{rel} \approx \frac{P_s M}{4}\left(\frac{1}{W}\right)^2\left(\frac{k_B T}{W}\right)^{3/4}. \tag{3}$$

Here P_s is the density of additional modes around the eigenvalue zero per mass unit (real number of modes, no factor of three!), M is the average atomic mass and W is the crossover energy between vibrational and tunnelling states at low temperatures.

The soft-potential model has been checked against the low-temperature glass anomalies in the heat capacity, the thermal conductivity and in the mechanical loss [14, 15]. The model predictions were found to be essentially correct, with an important exception: as soon as the barrier height of the double-well potentials begins to be a sizeable fraction of the thermal energy at the glass transition, the measured classical relaxation gets much weaker than the soft-potential prediction [28, 15]. As we will see, the same effect appears in our neutron spectra.

For the neutron data, one needs a suitable interpolation scheme between equation (1) below the boson peak and a slowly decreasing eigenvalue density above. As it turns out, it is convenient to use

$$p(\lambda) = \frac{3\lambda^{1/2}/2(\hbar\omega_D)^3 + a(\lambda/\lambda_c)^{3/2} + f_{rel}}{1 + (\lambda/\lambda_c)^b}. \tag{4}$$

Here a is the constant eigenvalue density above the boson peak and λ_c is the crossover eigenvalue. For a truly constant eigenvalue density at high eigenvalues, the exponent b must be

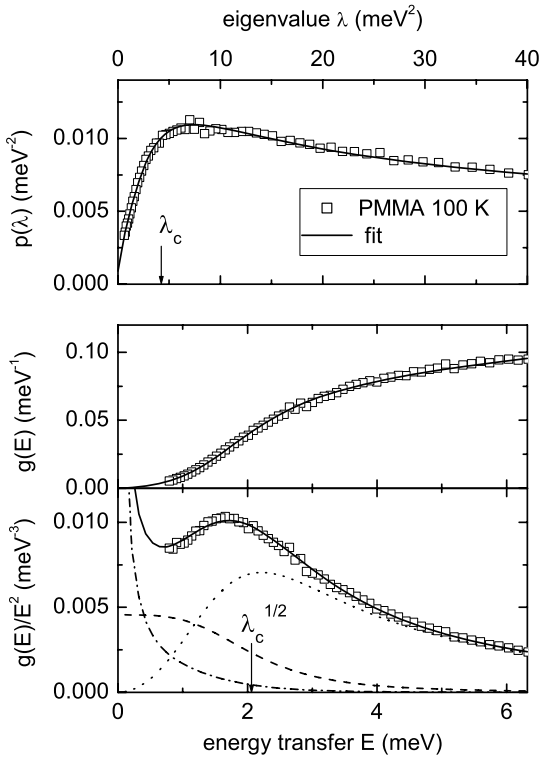

Figure 6. (a) Eigenvalue density in polymethylmethacrylate (PMMA) at 100 K, (b) same data and same fit in $g(E)$ and (c) same data and fit in $g(E)/E^2$, with the fit decomposed in sound waves (dashed line), additional vibrations (dotted line) and relaxation (dash–dotted line).

3/2; our fits required values between 1.6 and 2.7 in order to describe the slow decrease at high eigenvalues.

At the crossover eigenvalue λ_c, the sound-wave density of states is one half of the Debye value and decreases further with increasing eigenvalue. Similarly, the density of the excess modes at λ_c is $a/2$ and decreases further with decreasing eigenvalue. Thus λ_c marks indeed the crossover from the sound-wave regime at low eigenvalues to the excess-mode regime at high eigenvalues.

Equation (4) has four free parameters: the crossover eigenvalue λ_c, the eigenvalue density a, the exponent b and the relaxational scattering strength $f_{\rm rel}$. ω_D is not a free parameter, because it can be taken from ultrasonic and Brillouin data for silica [29], germania [30], B_2O_3 [31], selenium [32], polybutadiene [26], polystyrene and polymethylmethacrylate [33].

Equation (2) implies the following relation between a, λ_c and the soft-potential parameters:

$$\frac{a}{\lambda_c^{3/2}} = \frac{P_s M}{48}\left(\frac{1}{W}\right)^5. \tag{5}$$

The fit form is illustrated in figure 6 for the example of glassy PMMA at 100 K, showing the eigenvalue density in figure 6(a), the conventional frequency density of states $g(E)$ in figure 6(b) and $g(E)/E^2$ (the quantity nearest to the measured neutron spectrum itself, with the boson peak) in figure 6(c). For $g(E)/E^2$, the effective eigenvalue density of equation (4)

translates into

$$\frac{g(E)}{E^2} = \frac{3/(\hbar\omega_D)^3 + 2aE^2/\lambda_c^{3/2} + f_{rel}/E}{1 + (E^2/\lambda_c)^b}. \tag{6}$$

Figure 6(c) shows the decomposition of the three terms of this equation for the fit. Note that the relaxation, which was a constant term in $p(\lambda)$, is now proportional to $1/E$ in the neutron spectrum at low frequency. At higher frequency, it gets an additional cutoff by the denominator. λ_c is lying between the boson peak eigenvalue and the maximum in $p(\lambda)$.

4. Results and discussion

4.1. Boson peak and two-level states

As pointed out in the introduction, the soft-potential model [14, 15] and the almost constant eigenvalue density of the random-matrix concept [11] are intimately related. In fact, the soft-potential model deals with the following question: what happens to a constant eigenvalue density around the eigenvalue zero in the presence of linear perturbation terms? Since there is always a fourth-order term in the mode potential, most of the modes get pushed up into the neighbourhood of λ_c, thereby forming the boson peak of figure 6(c).

If this explanation for the boson peak is true, the eigenvalue density a at the crossover eigenvalue λ_c should be close to that at the eigenvalue zero, which feels the perturbation via the linear terms. How can one check that?

One possibility to do this is to rewrite equation (5), which formulates the pushing-up mechanism quantitatively, into the form

$$\frac{W}{\lambda_c^{1/2}} = \left(\frac{P_s M}{48 a \lambda_c}\right)^{1/5}. \tag{7}$$

One then has two ways of getting the ratio $W/\lambda_c^{1/2}$: the first one taking the value of W from the fit to the low-temperature anomalies and the value λ_c from the neutron fit, the second one by inserting $P_s M$ from the low-temperature fit and the product $a\lambda_c$ from the neutron fit into equation (7). Table 1 compares data for seven glasses obtained in this way. One finds excellent agreement between the values obtained directly and those obtained from the eigenvalue density ratio, with a ratio 1.03 ± 0.04. In fact, the accuracy is a bit surprising, because equation (4), used for the determination of a and λ_c, is no more than a pragmatic interpolation form.

From table 1, one draws three conclusions:

(i) the soft-potential explanation of the boson peak seems to be valid;
(ii) the ratio $W/\lambda_c^{1/2}$ differs from glass to glass;
(iii) The fit form of equation (4) for the crossover seems to be well chosen.

The last conclusion is further supported by low-temperature heat capacity data. Together with equation (2), equation (4) translates into a vibrational density of states

$$g(E) = \frac{3E^2/(\hbar\omega_D)^3 + P_s M E^4/24W^5}{1 + (E^2/\lambda_c)^b} \tag{8}$$

which no longer contains the eigenvalue density a. We insert this vibrational density of states into the empirical soft-potential expression for the low-temperature heat capacity C_p:

$$C_p = 10 P_s k_B \left(\frac{k_B T}{W}\right)^{1.2} + \frac{3k_B^2 T}{M} \int_0^\infty \frac{g(k_B T x) e^x x^2 \, dx}{(e^x - 1)^2} \tag{9}$$

where the first part is the tunnelling state contribution.

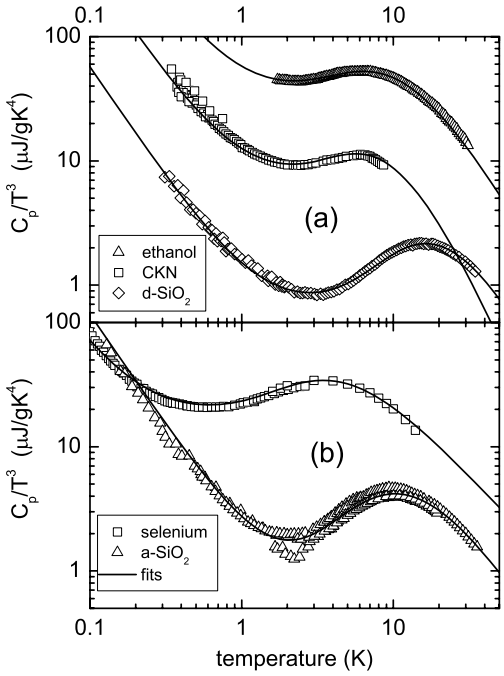

Figure 7. Heat capacity fits (continuous lines) in terms of equation (9) for (a) glassy ethanol [23], CKN [6] and densified silica [34], (b) silica [35] and selenium [36].

Table 1. Comparison to soft-potential parameters (PS = polystyrene, PMMA = polymethylmethacrylate, PB = 1,4-polybutadiene). P_s, C and W are taken from [15]; a, λ_c and b from the present work. T is the temperature of the neutron measurement. r_1 is the ratio $r = W/\lambda_c^{1/2}$ determined directly, r_2 is the ratio determined via equation (7). a_{sp} is calculated from equation (12).

Glass	SiO_2	GeO_2	B_2O_3	Se	PS	PMMA	PB
M (au)	20	34.86	14	78.96	6.5	6.66	5.4
$10^6 P_s M$	2.1	2.3	0.54	1.1	1.2	1.6	1.1
W (meV)	0.33	0.33	0.18	0.095	0.155	0.215	0.215
10^4 C	2.6	2.2	3.1	1.9	7.1	3.5	3.4
T (K)	100	300	300	100	35	40	50
$\hbar\omega_D$ (meV)	42.6	26.8	25.3	9.6	19.6	21.9	19.7
a (meV^{-2})	0.000 924	0.001 85	0.001 24	0.008 62	0.0015	0.000 993	0.001 34
λ_c (meV^2)	18.6	18.6	7.2	2.79	3.53	3.7	7.0
b	1.99	1.93	1.79	1.57	1.76	1.72	1.75
r_1	0.076	0.076	0.067	0.057	0.083	0.112	0.081
r_2	0.076	0.067	0.066	0.062	0.086	0.098	0.075
a/a_{sp}	0.76	1.08	1.41	0.85	1.26	0.60	1.14

Figure 7(a) shows fits with equation (9) to the measured heat capacities of glassy ethanol [23], $Ca_{0.4}K_{0.6}(NO_3)_{1.4}$ (CKN) [6] and densified silica [34]. Even the case of CKN, which has been argued to contradict the soft-potential model [6], is well fitted by the equation (the ability of the soft-potential model to describe the heat capacity of CKN has been demonstrated earlier [37]). Figure 7(b) shows the fit to the heat capacities of silica [35] and selenium [36].

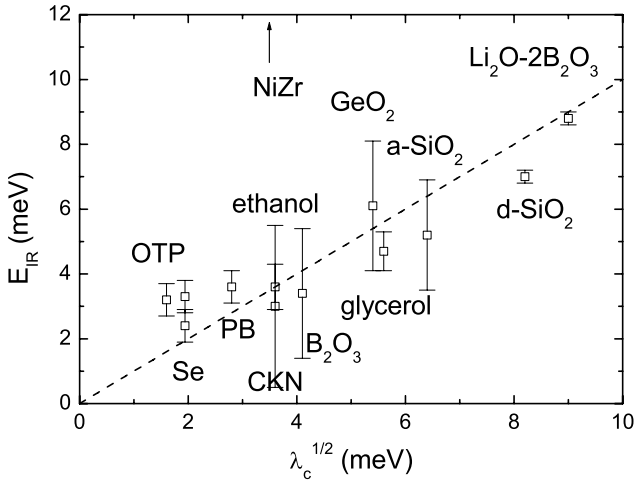

Figure 8. Ioffe–Regel limit frequencies from x-ray and neutron Brillouin data [9] plotted against the crossover frequency $\lambda_c^{1/2}$ for 12 glasses. The value for NiZr (22 meV) lies out of the range.

Table 2. Fit parameters of equation (9) to the low-temperature heat capacity data of figure 7.

Glass	a-SiO_2	d-SiO_2	CKN	C_2H_5OH	Se
M (au)	20	20	40.1	5.12	78.96
$\hbar\omega_D$ (meV)	42.5	46.8	16.7	20.0	9.6
$10^6 P_s M$	2.2	1.6	14.1	7.6	0.92
W (meV)	0.32	0.45	0.34	0.34	0.095
λ_c (meV^2)	18.7	67.3	13.0	14.1	2.25
b	1.95	2.5	3.0	2.1	1.66

The good fits in figures 7(a) and (b) show that the crossover parameter λ_c is able to adapt both the position and the height of the maximum in C_p/T^3, which is again an argument both for the validity of our soft-potential explanation of the boson peak and for the suitability of the interpolation form, equation (4).

Table 2 compiles the fit parameters of the heat capacity data in figure 7.

4.2. Ioffe–Regel limit

Though our definition of the crossover eigenvalue λ_c is in terms of a crossover in the vibrational density of states, one expects a close connection to the Ioffe–Regel limit, where the sound waves get overdamped.

Figure 8 compares fitted values of $\lambda_c^{1/2}$ to results obtained from x-ray and neutron Brillouin scattering [9, 10]. The crossover eigenvalues of a-SiO_2, GeO_2, B_2O_3, selenium and polybutadiene are taken from table 1; those of d-SiO_2, CKN and ethanol from table 2. The values for glycerol [21] OTP [20] and NiZr [10] were fitted to the neutron data in the literature; the value for Li_2O–$2B_2O_3$ to unpublished neutron data [40]. The error bars of these eigenvalues are small, much smaller than the error bars of the Ioffe–Regel limit in figure 8. Note that selenium has two data points: the lower one taken from neutron Brillouin data [39] and the higher one taken from x-ray Brillouin data [38].

There is one case, NiZr, where the x-ray values are much larger than $\lambda_c^{1/2}$ and which has been taken as evidence against the coincidence of the Ioffe–Regel limit and the boson peak [10]. This is a controversial topic [9, 10]. NiZr is not the only glass where the phonons above the boson peak have relatively low damping, lower than that calculated from the Ioffe–Regel criterion for their respective frequencies (remember that this limit increases linearly with frequency). OTP is another such case [9].

If we consider NiZr and OTP as outsiders, the rest fits nicely to the relation $E_{IR}/\lambda_c^{1/2} = 0.94 \pm 0.07$, indicating a Ioffe–Regel limit E_{IR} which is even a bit lower than the crossover of our interpolation formula, equation (4), again in surprisingly accurate agreement with a rather hazy expectation.

Let us see whether one can quantify the hazy expectation. The Ioffe–Regel limit is defined as the frequency at which the mean free path l (the length over which the amplitude of the sound wave decreases by the factor $1/e$) is equal to the wavelength. Let us start from the soft-potential equation (12) of [15]

$$l_{\mathrm{res,vib}}^{-1} = \frac{\pi\omega C_j}{v_j}\frac{1}{8}\left(\frac{\hbar\omega}{W}\right)^3, \tag{10}$$

where ω is the frequency of the sound wave, C is a dimensionless measure of the coupling between the sound wave and the excess mode, v is the sound velocity and the index j is l and t for longitudinal and transverse waves, respectively. Since the wavelength is $2\pi v_j/\omega$, the Ioffe–Regel limit frequency for longitudinal and transverse waves should be the same for $C_l = C_t$. In fact, one finds $C_l \approx C_t \approx C$, where C is an average value which can be fitted to the low-temperature thermal conductivity [15]. Assuming that the Ioffe–Regel limit lies indeed at λ_c, one gets the condition

$$\frac{\omega}{2\pi v_j} = \frac{\pi\omega C_j}{v_j}\frac{1}{16}\frac{\lambda_c^{3/2}}{W^3}. \tag{11}$$

The 16 in the denominator comes from the interpolation form, equation (4), according to which we have a factor of one half at λ_c. Again inserting equation (5), one finally gets an expression for a (here denoted a_{sp} to emphasize that it is calculated from the soft-potential model and our interpolation form, provided that λ_c is indeed the Ioffe–Regel limit):

$$a_{sp} = \frac{P_s M}{6\pi^2 C W^2}. \tag{12}$$

The ratio between the measured a and this soft-potential value a_{sp} is 0.97 ± 0.12 according to table 1, again a surprisingly good agreement.

Let us return to the questionable case in figure 8. If this idea works so well, why does it fail in NiZr? NiZr [10] shows clearly that one has well-defined sound waves above the crossover eigenvalue λ_c, well defined in the Ioffe–Regel sense that their width is smaller than their frequency divided by π. On the other hand, NiZr has a boson peak which looks exactly like the boson peak in other glasses (and is in fact nicely fitted by equation (4)).

NiZr is a metallic glass, which is relatively close to a frozen simple liquid. One expects only sound waves and nothing else, which is very different from the silica case, where the boson peak consists essentially of coupled SiO_4-tetrahedra librations [41]. Thus the approximately constant eigenvalue density above the crossover must consist, to a large extent, of phonons from the neighbourhood of the zone boundary. In fact, the modes show a kind of broadened dispersion curve up to and even exceeding the zone boundary, which is a common feature of metallic glasses. How can one reconcile this with a Ioffe–Regel limit at a rather low frequency?

In principle, this is not impossible. While the phonons above the crossover have a width lower than their Ioffe–Regel value, their width is still larger than the Ioffe–Regel width at the

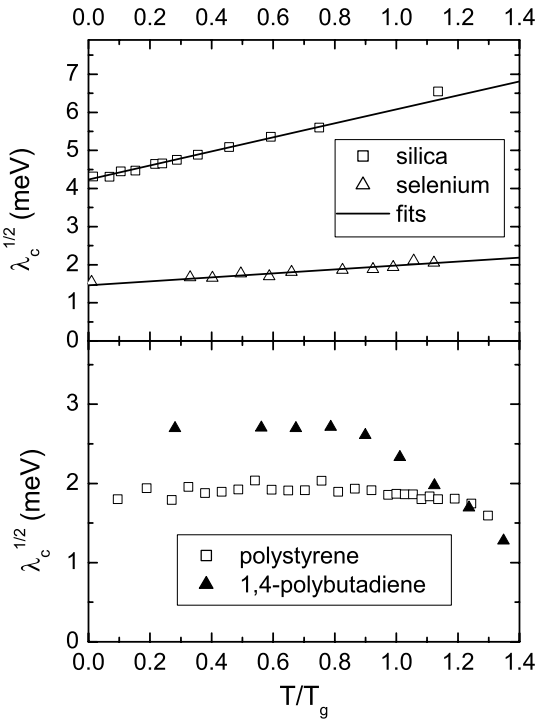

Figure 9. Temperature dependence of the crossover eigenvalue λ_c for (a) silica and selenium, (b) polybutadiene and polystyrene.

crossover. If one admits the possibility that the width stays approximately constant down to lower frequency, one could still have the Ioffe–Regel limit at the crossover. Such a behaviour has never been observed in glasses, but occurs in crystals with a low-lying resonant mode [42]. In order to check this possibility in NiZr, one should perform x-ray measurements with higher resolution, to see whether the width of the phonon at 3.4 meV is indeed as small as is given by the relatively poor resolution of the published measurements [10].

4.3. Temperature dependence

Figures 9(a) and (b) show the temperature dependence of the crossover frequency $\lambda_c^{1/2}$, plotted against the ratio T/T_g, where T_g is the glass temperature. In two cases, silica and selenium, the crossover eigenvalue increases with increasing temperature even beyond the glass temperature (figure 9(a)). Within the error bars, this increase is linear in temperature, which is consistent with a linear increase of the fourth-order term W in the excess mode potential. This in turn is consistent with the existence of a higher-order term, say an x^6 term in the mode displacement x, which becomes important with increasing mean square displacement (the mean square displacement increases essentially linearly with temperature in the glass phase).

The effect is absent in B_2O_3 and in the polymers. Polybutadiene and polystyrene are shown in figure 9(b). One observes an essentially constant λ_c (implying a constant W) until one approaches the glass transition. Then, λ_c decreases markedly in B_2O_3 and more markedly in polybutadiene than in polystyrene. In polymethylmethacrylate and polyisobutylene, where

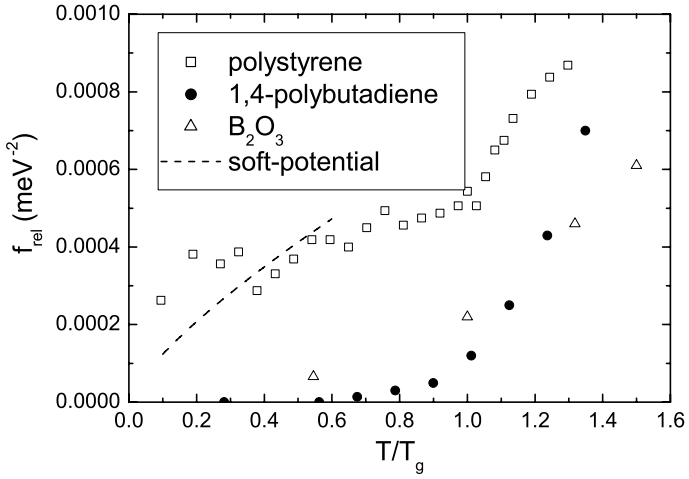

Figure 10. Temperature dependence of the relaxational scattering coefficient $f_{\rm rel}$ in B_2O_3, polybutadiene and polystyrene.

we have only glass phase data, λ_c stays temperature-independent within the error bars, even though the Debye frequency decreases markedly with increasing temperature.

Figure 9 demonstrates that the crossover eigenvalue does not depend on the Debye frequency. In silica, the Debye frequency increases by 2.5% as the temperature increases to the glass transition; in selenium it decreases by 13%. Nevertheless, both crossover eigenvalues increase, most probably by an anharmonic temperature effect. Interestingly, if one tries to explain the phonon hardening in silica by the hardening of the boson peak and the known interaction between sound waves and excess modes, one also fails. The interaction in our model accounts only for about one fifth of the observed Debye frequency shift. These two kind of modes are less dependent on each other than one usually thinks, so a perturbation treatment of their interaction seems feasible.

The eigenvalue density a is practically temperature-independent in all cases, with the exception of B_2O_3. There, one finds an increase in a by a factor of 1.4 in the glass phase, between 300 and 550 K (see figure 5). In the B_2O_3 liquid, a stays again constant. We have no explanation for this anomalous behaviour.

Figure 10 shows the temperature dependence of the relaxational part $f_{\rm rel}$ of the scattering in polystyrene, polybutadiene and B_2O_3. In principle, the soft-potential model predicts a relatively strong scattering already at low temperatures, increasing with temperature as $T^{0.75}$ (see equation (3)). In most cases, however, the observed relaxational scattering is weaker than the soft-potential prediction. An exception is polystyrene, where the relaxational component at low temperature even exceeds the soft-potential expectation (the dashed line in figure 10).

One needs temperatures above 50 K to perform a reasonable measurement. In the neutron measurement, one samples barriers about three times higher than the average thermal energy. This implies that one samples relatively large negative eigenvalues, which can have a different eigenvalue density. From ultrasonic data [15], one knows that the relaxations fall rapidly below the soft-potential expectation with rising temperature, consistent with the low values of $f_{\rm rel}$ observed in experiment. The advantage of the soft-potential formulation, however, is that one gets the correct spectral form of the relaxational scattering and thus gets rid of a disturbing influence.

5. Summary and conclusions

In this work, we fitted neutron spectra of seven glasses, silica, germania, selenium, boron trioxide and three polymers, in terms of an interpolation form. The form holds the promise of resembling the final theory for the vibrational density of states of glasses, a theory which is still missing. The form interpolates from a mixture of sound waves, resonant vibrational modes and relaxational modes at low frequency, described in terms of the soft-potential model [14, 15], to the more or less constant eigenvalue density of a random dynamical matrix at higher frequencies.

The interpolation form characterizes the sound waves by the Debye frequency ω_D, the high-frequency eigenvalue density by a free parameter a and the crossover between the two regions by a crossover eigenvalue λ_c. An additional dimensionless parameter b is needed to describe a decrease in the eigenvalue density towards higher eigenvalues, which is found not only in the seven glasses of the present work, but also in all available literature data.

The fits show that the fitted high-frequency eigenvalue density a is consistent with the soft-potential parameters P_s and W. In fact, a can be calculated from the two soft-potential parameters and the crossover eigenvalue (see table 1).

There is a third dimensionless soft-potential parameter, C, which characterizes the interaction between excess modes and sound waves. Using this parameter value from soft-potential fits of the low-temperature glass anomalies, one predicts, on the basis of our interpolation form, that the fitted crossover eigenvalues should be close to the Ioffe–Regel limit of strong damping of the sound waves, where the mean free path equals the wavelength. A comparison with x-ray and neutron Brillouin data of 12 glasses (figure 8) shows that this is indeed true in nine cases.

The results indicate that one needs a theory which interpolates from sound waves to a random-matrix solution. The theory should provide an interpolation which is close to our pragmatic form, equation (4). In addition, the theory should explain why the eigenvalue density tends to decrease toward higher eigenvalues. This might be the influence of the vibrational entropy, which tends to push the eigenvalues downward. This influence is not taken into account in any of the existing theories and models [1–8].

Acknowledgment

We thank Aleksandar Matic for supplying the Li_2O–$2B_2O_3$ boson peak data prior to publication and for helpful controversial discussions.

References

[1] Gurevich V L, Parshin D A and Schober H R 2003 *Phys. Rev.* B **67** 094203
[2] Schirmacher W, Diezemann G and Ganter C 1998 *Phys. Rev. Lett.* **81** 136
[3] Taraskin S N, Loh Y L, Natarajan G and Elliott S R 2001 *Phys. Rev. Lett.* **86** 1255
[4] Nakayama T 2002 *Rep. Prog. Phys.* **65** 1195
[5] Götze W and Mayr M R 2000 *Phys. Rev.* E **61** 587
[6] Sokolov A P, Calemczuk R, Salce B, Kisliuk A, Quitmann D and Duval E 1997 *Phys. Rev. Lett.* **78** 2405
[7] Grigera T S, Martin-Mayor V, Parisi G and Verrocchio P 2002 *J. Phys.: Condens. Matter* **14** 2167
[8] Scopigno T, Pontecorvo E, Di Leonardo R, Krisch M, Monaco G, Ruocco G, Ruzicka B and Sette F 2003 *J. Phys.: Condens. Matter* **15** S1269
[9] Rufflé B, Guimbretiere G, Courtens E, Vacher R and Monaco G 2006 *Phys. Rev. Lett.* **96** 045502 ; the x-ray damping data for OTP in this paper are a factor of 2 too high (private communication by G Monaco)
[10] Scopigno T, Suck J-B, Angelini R, Albergamo F and Ruocco G 2006 *Phys. Rev. Lett.* **96** 135501

[11] Wigner E P 1958 *Ann. Math.* **67** 325
[12] Schirmacher W 2006 private communication
[13] Phillips W A (ed) 1981 *Amorphous Solids: Low Temperature Properties* (Berlin: Springer)
[14] Parshin D A 1994 *Phys. Solid State* **36** 991
[15] Ramos M A and Buchenau U 1997 *Phys. Rev.* B **55** 5749
[16] Fabiani E, Fontana A and Buchenau U 2006 unpublished
[17] Schober H, Strauch D, Nützel K and Dorner B 1993 *J. Phys.: Condens. Matter* **5** 6155
[18] Buchenau U, Prager M, Nücker N, Dianoux A J, Ahmad N and Phillips W A 1986 *Phys. Rev.* B **34** 5665
[19] Meyer A, Wuttke J, Petry W, Peker A, Bormann R, Coddens G, Kranich L, Randl O G and Schober H 1996 *Phys. Rev.* B **53** 12107
[20] Tölle A, Zimmermann H, Fujara F, Petry W, Schmidt W, Schober H and Wuttke J 2000 *Eur. Phys. J.* B **16** 73
[21] Wuttke J, Hernandez J, Li G, Coddens G, Cummins H Z, Fujara F, Petry W and Sillescu H 1994 *Phys. Rev. Lett.* **72** 3052
[22] Chumakov A I, Sergueev I, van Bürck U, Schirmacher W, Asthalter T, Rüffer R, Leupold O and Petry W 2004 *Phys. Rev. Lett.* **92** 245508
[23] Talon C, Ramos M A, Vieira S, Cuello G J, Bermejo F J, Criado A, Senent M L, Bennington S M, Fischer H E and Schober H 1998 *Phys. Rev.* B **58** 745
[24] Sarkar S K, Matharoo G S and Pandey A 2004 *Phys. Rev. Lett.* **92** 215503
[25] Phillips W A, Buchenau U, Nücker N, Dianoux A J and Petry W 1989 *Phys. Rev. Lett.* **63** 2381
[26] Zorn R, Arbe A, Colmenero J, Frick B, Richter D and Buchenau U 1995 *Phys. Rev.* E **52** 781
[27] Engberg D, Wischnewski A, Buchenau U, Börjesson L, Dianoux A J, Sokolov A P and Torell L M 1998 *Phys. Rev.* B **58** 9087
[28] Keil R, Kasper G and Hunklinger S 1993 *J. Non-Cryst. Solids* **164–166** 1183
[29] Bucaro J A and Dardy H D 1974 *J. Appl. Phys.* **45** 5324
[30] Zeller R C and Pohl R O 1971 *Phys. Rev.* B **4** 2029
[31] Grimsditch M and Torell L M 1989 *Dynamics of Disordered Materials* (*Springer Proceedings in Physics* vol 37) ed D Richter, A J Dianoux, W Petry and J Texeira (Berlin: Springer) p 196
[32] Galli G, Migliardo P, Bellissent R and Reichardt W 1986 *Solid State Commun.* **57** 195
[33] Krüger H 1989 *Optical Techniques to Characterize Polymer Systems* (*Studies in Polymer Science* vol 5) ed H Bässler (Amsterdam: Elsevier) p 491
[34] Liu X, von Löhneysen H C, Weiss G and Arndt J 1995 *Z. Phys.* B **99** 49
[35] Flubacher P, Leadbetter A J, Morrison J A and Stoicheff B P 1959 *J. Phys. Chem. Solids* **12** 53
Zeller R C and Pohl R O 1971 *Phys. Rev.* B **4** 2029
von Löhneysen H C, Rüsing H and Sander W 1985 *Z. Phys.* B **60** 323
Buchenau U, Prager M, Nücker N, Dianoux A J, Ahmad N and Phillips W A 1986 *Phys. Rev.* B **34** 5665
[36] Lasjaunias J C 1969 *Compt. Rend.* **269** 763
Brand O and von Löhneysen H C 1991 *Europhys. Lett.* **16** 455
[37] Ramos M A 2004 *Phil. Mag.* **84** 1313
[38] Scopigno T, DiLeonardo R, Ruocco G, Baron A Q R, Tsutsui S, Bossard F and Yannopoulos S N 2004 *Phys. Rev. Lett.* **92** 025503
[39] Foret M, Hehlen B, Taillades G, Courtens E, Vacher R, Casalta H and Dorner B 1998 *Phys. Rev. Lett.* **81** 2100
[40] Matic A 2006 private communication
[41] Hehlen B, Courtens E, Vacher R, Yamanaka A, Kataoka M and Inoue K 2000 *Phys. Rev. Lett.* **84** 5355
[42] Zinken A, Buchenau U, Fenzl H J and Schober H R 1977 *Solid State Commun.* **22** 693